CHAPTER III
REFORMING OF CO_2-CONTAINING NATURAL GAS USING AN AC GLIDING ARC SYSTEM: EFFECT OF GAS COMPONENTS IN NATURAL GAS*

3.1 Abstract

The objective of the present work was to study the reforming of simulated natural gas via the nonthermal plasma process with the focus on the production of hydrogen and higher hydrocarbons. The reforming of simulated natural gas was conducted in an alternating current (AC) gliding arc reactor under ambient conditions. The feed composition of the simulated natural gas contained a CH_4:C_2H_6:C_3H_8:CO_2 molar ratio of 70:5:5:20. To investigate the effects of all gaseous hydrocarbons and CO_2 present in the natural gas, the plasma reactor was operated with different feed compositions: pure CH_4, CH_4/He, CH_4/C_2H_6/He, CH_4/C_2H_6/C_3H_8/He and CH_4/C_2H_6/C_3H_8/CO_2. The results showed that the addition of gas components to the feed strongly influenced the reaction performance and the plasma stability. In comparisons among all the studied feed systems, both hydrogen and C_2 hydrocarbon yields were found to depend on the feed gas composition in the following order: CH_4/C_2H_6/C_3H_8/CO_2 > CH_4/C_2H_6/C_3H_8/He > CH_4/C_2H_6/He > CH_4/He > CH_4. The maximum yields of hydrogen and C_2 products of approximately 35 and 42%, respectively, were achieved in the CH_4/C_2H_6/C_3H_8/CO_2 feed system. In terms of energy consumption for producing hydrogen, the feed system of the CH_4/C_2H_6/C_3H_8/CO_2 mixture required the lowest input energy, in the range of 3.58×10^{-18}- 4.14×10^{-18} W·s (22.35-25.82 eV) per molecule of produced hydrogen.

Keywords: Natural gas reforming; Gliding arc discharge; Plasma

---

*Published in Plasma Chemistry and Plasma Processing (2007), 27(5), 559-576.

3.2 Introduction

Natural gas generally contains a large amount of methane and significant quantities of ethane, propane, carbon dioxide and nitrogen. In different parts of the world, the composition of natural gas varies considerably according to the different conditions. Interestingly, natural gas resources with high concentrations of carbon dioxide have been found in abundance in several areas, especially in Southeast Asia, including Thailand. Taking into account this point of view, the reforming of methane with carbon dioxide (Equation 3.1) is a promising way to directly utilize the natural gas, of which both methane and carbon dioxide are major constituents, without any prior separation process, resulting in it being more economical in terms of cutting down the high cost of an additional separation unit and reducing the net emission of carbon dioxide as a greenhouse gas.

$$CH_4 + CO_2 \rightarrow 2CO + 2H_2 \quad \Delta H_{298K} = 2.05 \times 10^{-19}\ W.s/H_2\text{-molecule} \qquad (3.1)$$

Research on the natural gas conversion to useful chemicals and fuels using various catalysts has been extensively done [1-7]. However, these studies have still faced two main difficulties: 1) the conventional catalytic reactions of natural gas require high operating temperatures, due to the presence of methane, a major component of natural gas, which is a very stable molecule with a strong C-H bond, and 2) the formation of coke deposition on the surface of spent catalysts, causing their rapid deactivation. Up to now, no catalyst is favorable for effectively inhibiting the coke formation in the industrial reforming of methane with CO_2.

Non-thermal plasma processes are considered to be attractive alternatives for converting natural gas into more valuable products at lower temperatures with no special quenching, and they can overcome the drawbacks of conventional catalytic reactions as mentioned above. Non-thermal plasma has non-equilibrium properties, which are commonly characterized by having a very high electron temperature while at the same time having a very low bulk gas temperature in the plasma zone. Under the non-thermal plasma environment, the gas molecules are basically activated to create highly active species (electrons, positive/negative ions and free radicals) for

both the initiation and the propagation of the chemical reactions. Therefore, a number of research studies have attempted to achieve the higher performance of methane reforming with CO_2 using different types of non-thermal plasmas [8-17]. A gliding arc is a new discharge type of non-thermal plasma which successfully provides the most effective non-equilibrium characteristics with simultaneously high productivity and good selectivity. Gliding arc plasma can be easily generated by applying an electrical discharge across a pair of electrodes having a special configuration. It is comprised of at least two diverging knife-shaped electrodes, which are positioned in a rapid gas flow. A high voltage is applied across the electrodes and provides the necessary electric field to break down the gas molecules passing between the electrodes and the discharge. The gliding arc discharge is initially generated through the gas flow at the narrowest gap distance between the electrodes, and then spreads by gliding progressively along and between the knife-shaped electrodes in the direction of the gas flow until it extinguishes by itself. Another new discharge promptly forms again at the initial point, after the voltage in the gap reaches the breakdown value [18,19]. According to its simplicity in configuration, as mentioned above, several research groups have increasingly employed this plasma reactor type for pollution control [20-24], surface treatment [25-27] and fuel conversion [28-34].

The objective of this research was to investigate natural gas reforming under non-thermal gliding arc discharge and was concerned with the concept of direct utilization of raw natural gas with a high CO_2 content. The effects of all of the gas components in natural gas on methane conversion and product selectivities were investigated experimentally to contribute comprehensive knowledge of the interactions among the gas components of natural gas under plasma reforming conditions. Comparative results of methane conversion, product yield and specific energy consumption in each feed system are also described systematically in this paper.

3.3 Experimental

3.3.1 AC Gliding Arc Discharge System

The flow rates of reactant gases were regulated by a set of mass flow controllers and transducers supplied by SIERRA® Instrument, Inc. A 7-μm in-line filter was placed upstream of each mass flow controller in order to trap any foreign particles. A check valve was placed downstream of each mass flow controller to prevent any back flow of the reactant gas. All of the reactant gases were well mixed inside a mixing chamber before being introduced upward to the gliding arc reactor.

The configuration of the AC gliding arc reactor and the experimental set-up of the studied plasma system are shown in Figures. 3.1 and 3.2, respectively. The gliding arc reactor was made of a glass tube with 9 cm OD and 8.5 cm ID, and has two diverging knife-shaped electrodes that were fabricated from stainless steel sheets with 1.2 cm width of each electrode. These electrodes were vertically positioned inside the reactor and connected to the power supply with four stainless steel rods. The gap distance between the pair of electrodes was fixed at 6 mm. Two teflon sheets were placed at the top and bottom of the electrodes to force the reactant gases to pass through the plasma zone. The two ends of reactor were sealed with two neoprene rubber stoppers. The studied system was conducted at atmospheric pressure

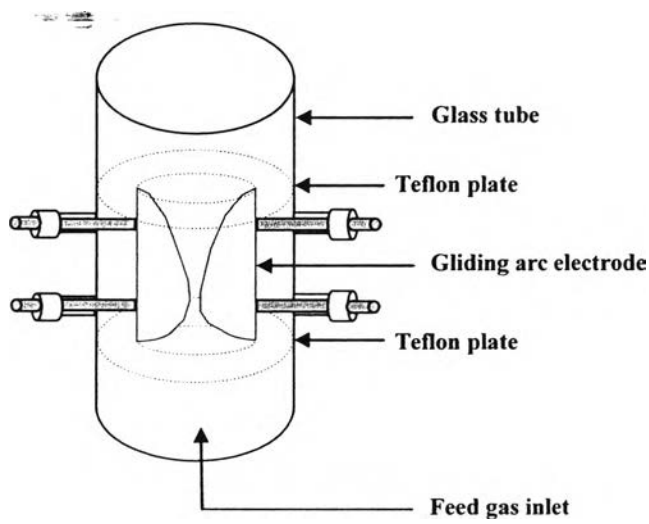

Figure 3.1 Configuration of a gliding arc plasma reactor.

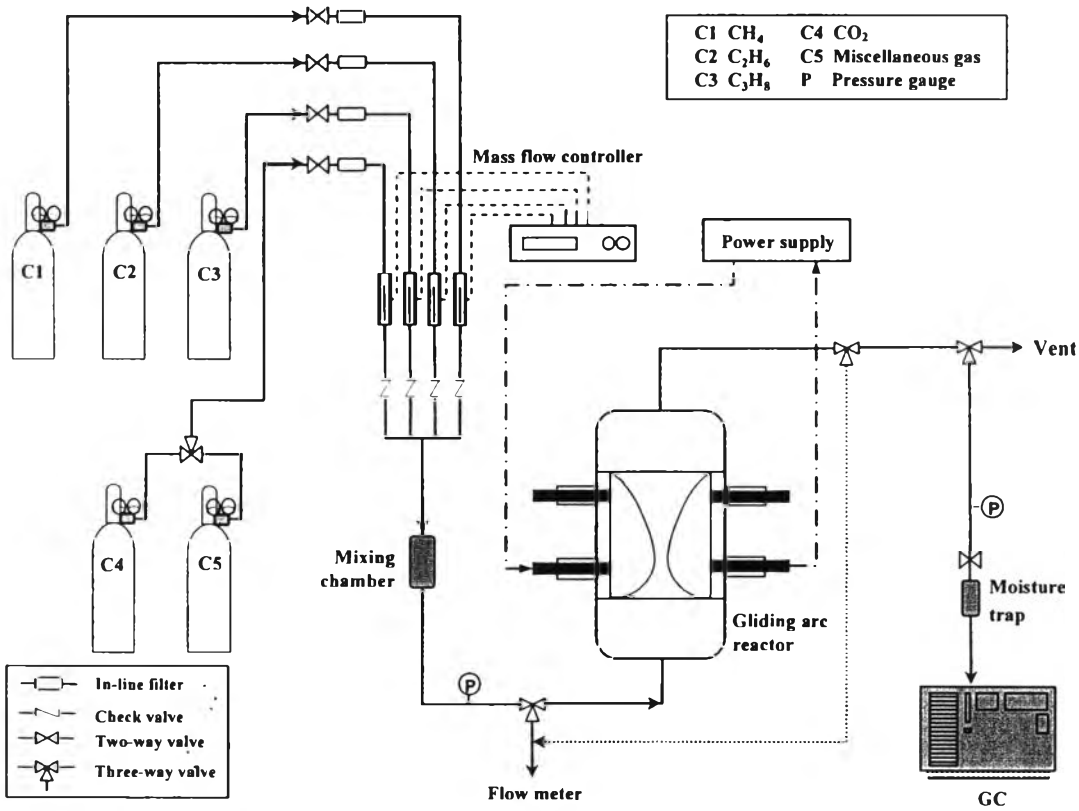

Figure 3.2 Experimental set-up of the gliding arc plasma system.

and ambient temperature. The compositions of the feed gas mixture and the outlet gas were analyzed by an on-line gas chromatograph (HP, 5890). A Carboxen 1000 packed column connected to a thermal conductivity detector (TCD) was used to detect H_2, N_2, O_2, CO, CH_4, CO_2, C_2H_2, C_2H_4, and C_2H_6. A PLOT Al_2O_3 "S" deactivated capillary column connected to a flame ionization detector (FID) was used to detect all small and large hydrocarbon molecules.

The power supply function consisted of three steps. For the first step, the domestic AC input of 220 V and 50 Hz was converted to a DC output of 70 V by a DC power supply converter. For the second step, a 500 W power amplifier with a function generator was used to transform the DC into AC current with a sinusoidal waveform and different frequencies. For the third step, the outlet voltage was stepped up by using a high voltage transformer. The output voltage and frequency were controlled by the function generator. The voltage and current at the low voltage side were measured instead of those at the high voltage side since the plasma generated is

non-equilibrium in nature. The high side voltage and current were thereby calculated by multiplying and dividing by a factor of 130, respectively. A power analyzer was used to measure power, power factor, current, frequency, and voltage at the low voltage side of the power supply unit.

3.3.2 Feed Gas Systems and Procedure

A series of experiments in this work were performed under different feed gas systems: pure methane, CH_4/He, CH_4/C_2H_6/He, $CH_4/C_2H_6/C_3H_8$/He and $CH_4/C_2H_6/C_3H_8/CO_2$. Methane (CH_4) with 99.99% purity, ethane (C_2H_6) with 99.5% purity, and propane (C_3H_8) with 99.5% purity were supplied by Thai Industrial Gas (Public) Co., Ltd. Carbon dioxide (CO_2) with 99.99% purity and helium (He) with 99.995% purity were supplied by Praxair (Thailand) Co., Ltd. In order to determine the effect of each component in the natural gas, each gas component was added one by one. Table 4.1 shows the molar compositions of the different feed systems used in the present study. The experiment was started with pure methane. After that, helium was added to obtain a constant methane-to-helium feed molar ratio of 70:30. Next, ethane, propane and CO_2 were added consecutively in order to obtain the required molar ratios of each feed system. In order to determine the effects of each gas component in the feed, the gliding arc system was operated by varying the feed flow rate, while the frequency, applied voltage, and electrode gap distance were kept constant. For any studied conditions, the feed was introduced into the gliding arc system without turning on the power unit. After the composition of outlet gas was invariant with time, the power unit was turned on. The outlet gas composition was analyzed every 30 min by the on-line GC. After the system reached steady state, the analysis of outlet gas composition was taken at least a few times for every one-hour interval. The experimental data were averaged to assess the process performance. During the experiments, the temperature at the reactor wall was found to be in the range of 150-200°C. Since the volume of the reactor outlet zone is rather large, the outlet gas was cooled close to room temperature. Both the flow rates of the feed and of the outlet were measured by using a bubble flow meter because of the gas volume change after the reaction.

Table 3.1 Gas compositions and feed molar ratios of all studied feed systems

Feed gas composition	Feed molar ratio
Pure CH_4	-
CH_4:He	70:30
CH_4:C_2H_6:He	70:5:25
CH_4:C_2H_6:C_3H_8:He	70:5:5:20
CH_4:C_2H_6:C_3H_8:CO_2	70:5:5:20

3.3.3 Reaction Performance Evaluation

The conversion is defined as:

$$\% \text{ Reactant conversion} = \frac{(\text{mole of reactant in} - \text{mole of reactant out})\,(100)}{\text{mole of reactant in}} \qquad (3.2)$$

The selectivities for C-containing products are defined on the basis of the amount of C-containing reactants converted from the reactants into any specified product as stated in Equation 3.3. In the case of hydrogen product, its selectivity is calculated based on H-containing reactants converted as stated in Equation 3.4:

$$\% \text{ Selectivity for any hydrocarbon product} = [P]\,(C_P)\,(100) / \Sigma\,[R]\,(C_R) \qquad (3.3)$$

where $[P]$ = moles of product in outlet gas stream

$[R]$ = moles of each reactant in feed stream to be converted

C_P = number of carbon atoms in a product molecule

C_R = number of carbon atoms in each reactant molecule

$$\% \text{ Selectivity for hydrogen} = [P]\,(H_P)\,(100) / \Sigma\,[R]\,(H_R) \qquad (3.4)$$

where H_P = number of hydrogen atoms in a product molecule

H_R = number of hydrogen atoms in each reactant molecule

The product yield is formulated as follows:

$$\% \text{ } C_2 \text{ hydrocarbons yield} = \Sigma (\% \text{ conversion of } CH_4, C_2H_6, C_3H_8, CO_2) \Sigma (\% \text{ selectivity for } C_2H_2, C_2H_4, C_2H_6) / (100) \quad (3.5)$$

$$\% \text{ } H_2 \text{ yield} = \Sigma (\% \text{ conversion of } CH_4, C_2H_6, C_3H_8) (\% \text{ selectivity for } H_2) / (100) \quad (3.6)$$

The specific energy consumption is calculated in a unit of W·s per a C-containing reactant molecule converted or per a hydrogen molecule produced (W·s/M) using the following equation:

$$\text{Specific energy consumption} = (P)(60) / (\tilde{N})(M) \quad (3.7)$$

where P = power (W)

$\tilde{N}$ = Avogadro's number (6.02×10^{23} molecules·g-mole^{-1})

M = rate of converted carbon in feed or rate of produced hydrogen molecule (g-mole·min^{-1})

3.4 Results and Discussion

3.4.1 Pure Methane Feed System

The results of the pure methane feed system as a function of feed flow rate are shown in Figure 3.3. The feed flow rate was varied from 25 to 150 cm^3/min, corresponding to the residence time in the range of 7.71-1.28 s. An increase in the feed flow rate results in lowering residence time in the plasma reaction zone and, therefore, the probability of collision between methane molecules and highly energetic electrons decreases, causing the largely decreasing methane dissociation or conversion and the yield of H_2 and C_2 products, as shown in Figure 3.3(a). From Figure 3.3(b), the concentrations of H_2 and C_2 products (C_2H_2, C_2H_4, and C_2H_6) decrease sharply with increasing feed flow rate up to 75 cm^3/min and then reach minimum values at very high feed flow rates. The main gas products were H_2, C_2H_2,

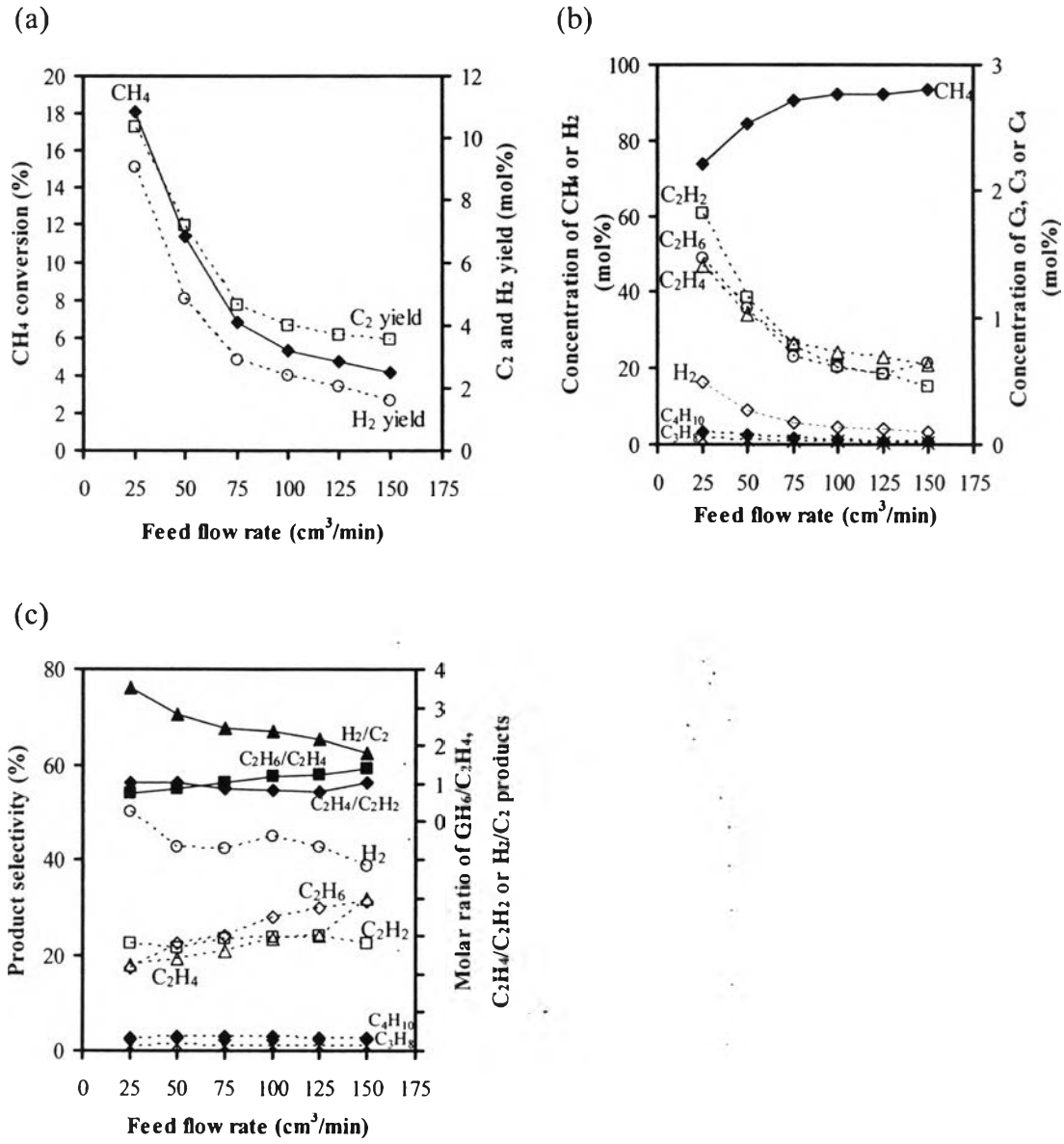

Figure 3.3 Effect of feed flow rate on (a) CH_4 conversion and product yields, (b) concentrations of outlet gas, and (c) product selectivities of pure methane feed system (applied voltage, 15.5 kV; frequency, 200 Hz; and electrode gap distance, 6 mm).

C_2H_4, and C_2H_6. Other hydrocarbon products, C_3H_8 and C_4H_{10}, were also detected in very small amounts lower than 0.05%. Interestingly, hydrocarbons higher than C_4 were not detected. For any given feed flow rate, the concentrations of gaseous products were in the following order: $H_2 > C_2H_6 \approx C_2H_4 \approx C_2H_2 > C_3H_8 \approx C_4H_{10}$. Figure 3.3(a) shows that at the lowest feed flow rate (25 cm^3/min), the highest yields

of H_2 and C_2 products are approximately 9 and 11%, respectively. Under this pure methane feed system, the hydrogen selectivity was much higher than the other products for all feed flow rates (Figure 3.3(c)), and the molar ratio of H_2 to C_2 products was approximately 2-3.5, suggesting that hydrogen is a primary product, which may be derived from the three main plausible reactions: (1) the dissociation of methane by electrons (Equations 3.8-3.11), (2) the dehydrogenation of ethane and ethylene (Equations 3.20-3.21), which are successively derived from coupling reactions of active species derived from methane dissociations (Equations 3.12-3.19), and (3) the cracking reaction of methane (Equation 3.22). The methane cracking reaction is verified by the presence of a large amount of coke deposit on the electrode surface and the inner reactor glass wall after running the plasma system for a long period of time.

Dissociation reactions of methane;

$$e^- + CH_4 \rightarrow CH_3 + H + e^- \quad (3.8)$$

$$e^- + CH_3 \rightarrow CH_2 + H + e^- \quad (3.9)$$

$$e^- + CH_2 \rightarrow CH + H + e^- \quad (3.10)$$

$$H + H \rightarrow H_2 \quad (3.11)$$

Coupling reactions of active species derived from methane dissociations;

$$CH_3 + CH_3 \rightarrow C_2H_6 \quad (3.12)$$

$$CH_3 + CH_2 + H \rightarrow C_2H_6 \quad (3.13)$$

$$CH_3 + CH \rightarrow C_2H_4 \quad (3.14)$$

$$CH_2 + CH_2 \rightarrow C_2H_4 \quad (3.15)$$

$$CH_2 + CH + H \rightarrow C_2H_4 \quad (3.16)$$

$$CH + CH \rightarrow C_2H_2 \quad (3.17)$$

$$CH_3 + CH_3 + CH_2 + CH_2 \rightarrow C_4H_{10} \quad (3.18)$$

$$CH_3 + CH_3 + CH_2 \rightarrow C_3H_8 \quad (3.19)$$

Dehydrogenation reactions of products derived from coupling reactions;

$$C_2H_6 \rightarrow C_2H_4 + H_2 \quad (3.20)$$

$$C_2H_4 \rightarrow C_2H_2 + H_2 \quad (3.21)$$

Cracking reaction of methane;

$$CH_4 \rightarrow C + 2H_2 \qquad (3.22)$$

As clearly noticed in Figure 3.3(c), with increasing feed flow rate, the H_2 selectivity tends to decline. The results are in good agreement with the work conducted by Holmen *et al.* [33]. In contrast, the selectivities for C_2H_6 and C_2H_4 slightly increased at higher feed flow rates while that for C_2H_2 was fairly constant at about 20%. The results imply that the methane cracking reaction favors at longer reaction times, whereas the coupling reactions of radicals forming C_2 products favor at shorter reaction times or higher feed flow rates. This is because the methane cracking reaction requires a higher energy than the methane coupling and dehydrogenation reactions. Additionally, the selectivities for C_3H_8 and C_4H_{10} were very low and remained nearly constant throughout the studied range of feed flow rates. The reactions to form C_3H_8 and C_4H_{10} possibly result from the coupling of various radicals derived from the methane dissociation. For a comparison among all C_2 products, there were no significant differences in their selectivities and concentrations at the same flow rates because the molar ratios of C_2H_6/C_2H_4 and C_2H_4/C_2H_2 were quite close to one, indicating that the rates of C_2H_6, C_2H_4, and C_2H_2 formation are almost the same. As shown in Figure 3.3(c), the molar ratio of H_2 to C_2 products is in the range of 1.8-3.5, and it decreases with increasing feed flow rate, indicating that the cracking reaction of methane occurs with much more difficulty than the methane dissociation, methane coupling, and dehydrogenation reactions.

3.4.2 CH_4/He Feed System

This experiment was conducted to investigate the effect of added helium on the plasma reforming reactions of methane at a CH_4:He feed molar ratio of 70:30. The CH_4/He feed system was operated at different feed flow rates in the range of 50 to 150 cm^3/min at a fixed gap distance of 6 mm. The methane conversion decreases slightly with increasing feed flow rate, as shown in Figure 3.4(a). The decrease in methane conversion is because an increase in feed flow rate leads to a shorter residence time, which, in turn, leads to a lower methane conversion, as already stated before. Although both the H_2 and C_2 yields showed similar trends to

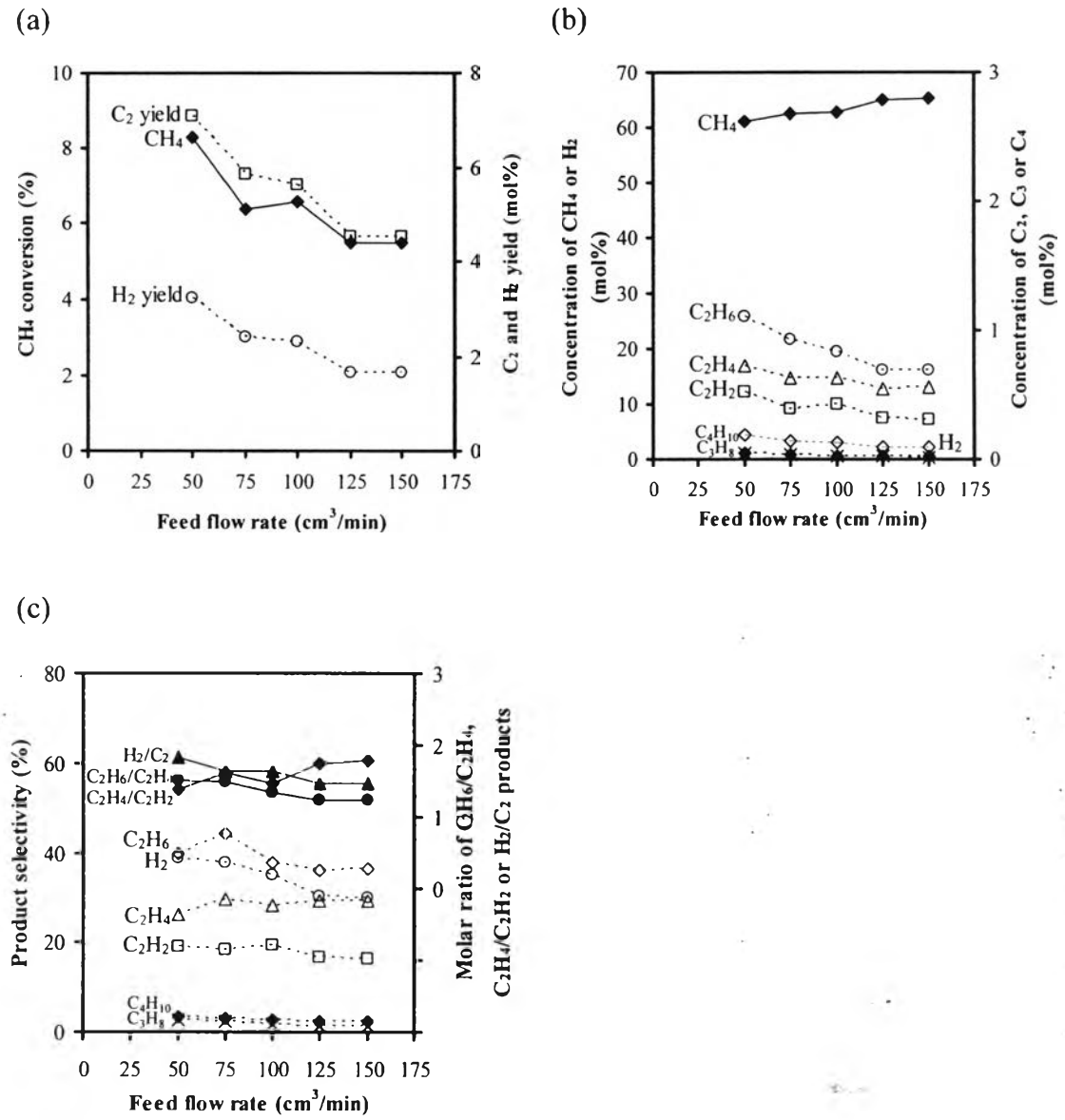

Figure 3.4 Effect of feed flow rate on (a) CH_4 conversion and product yields, (b) concentrations of outlet gas, and (c) product selectivities of methane/helium feed system (applied voltage, 15.5 kV; frequency, 200 Hz; and electrode gap distance, 6 mm).

the CH_4 conversion, the C_2 yield was much higher than the H_2 yield. Figure 3.4(b) shows the outlet gas concentrations as a function of the feed flow rate. The concentration of methane in the reactor outlet stream increased gradually with increasing feed flow rate. The concentrations of all higher hydrocarbon products and H_2 slowly decreased with increasing feed flow rate up to 125 cm^3/min and then

remained almost constant. The concentrations of C_3H_8 and C_4H_{10} decreased slightly as the feed flow rate increased, and they were very low. The result indicates that the feed flow rate has little effect on the production of C_3H_8 and C_4H_{10}. Figure 3.4(c) shows the product selectivities and the molar ratio of H_2 to all C_2 products as a function of feed flow rate. The selectivities for C_2H_6 and H_2 decreased with increasing feed flow rate while the selectivities for C_2H_4, C_2H_2, C_3H_8, and C_4H_{10} remained unchanged with feed flow rate. The molar ratios of H_2/C_2 products, C_2H_6/C_2H_4, and C_2H_4/C_2H_2 did not vary with feed flow rate. For the CH_4/He feed system, the concentrations of gaseous products were in the following order: $H_2 > C_2H_6 > C_2H_4 > C_2H_2 > C_3H_8 \approx C_4H_{10}$.

For a comparison between these two feed systems, pure methane and methane/helium, the presence of helium in the feed had a positive effect on the system by promoting the stability of plasma by remarkably reducing carbon formation on the electrode surface and on the inner glass wall of the reactor. From the observation and the calculation of carbon balance, carbon formation was found to be less than 1% for the methane/helium feed system while a larger amount of coke clearly appeared in the pure methane feed system, particularly at low feed flow rates. Figure 3.4(c) shows that the selectivities for all C_2 products did not change significantly over the studied range of feed flow rate, while the selectivities for C_3H_8 and C_4H_{10} hydrocarbons decreased slightly with increasing feed flow rate. This result implies that the feed flow rate plays an insignificant role on product selectivities in the CH_4/He feed system. Interestingly, the C_2H_6/C_2H_4 molar ratio was greater than one, indicating that the formation rate of C_2H_6 is higher than the formation rate of C_2H_4. In addition, the molar ratio of H_2/C_2 products was found to be lower than 2 for this feed system while it was about 2-3 for the pure methane feed. This might be attributed to a higher formation rate of C_2H_6, thus leading to the higher values of C_2H_6 selectivity among all products at any given feed flow rate. Ethane was the main product in the CH_4/He feed system, suggesting that in the presence of He, the coupling reaction of methane via methyl radicals to form ethane may have a higher probability of occurring than the other reactions, as compared to the pure methane feed system.

Furthermore, in the case of the methane/helium system at any given feed flow rate, concentrations and selectivities of C_2 products showed a noticeable difference in values for C_2H_6, C_2H_4, and C_2H_2 ($C_2H_6 > C_2H_4 > C_2H_2$). The obtained results imply that C2H6 is mostly dehydrogenated to form C_2H_4 and H_2, and C_2H_4 may be further dehydrogenated to form C_2H_2 and H_2, as confirmed by the molar ratios of H_2/C_2, C_2H_6/C_2H_4, and C_2H_4/C_2H_2 remained nearly constant in the narrow range of about 1-2 throughout the studied feed flow rate range.

3.4.3 CH_4/C_2H_6/He Feed System

This experiment was designed to investigate the effect of added ethane on the plasma reforming reactions of methane with a CH_4:C_2H_6:He feed molar ratio of 70:5:25. The feed flow rate was varied from 50 to 150 cm^3/min, corresponding to a residence time in the range of 3.86 to 1.28 s. Figure 3.5 shows the results of the plasma reforming reactions of the CH_4/C_2H_6/He feed system at different feed flow rates. From Figure 3.5(a), with increasing feed flow rate, both CH_4 and C_2H_6 conversions decrease as expected, and the H_2 and C_2 product yields appear to drop remarkably. The conversion of C_2H_6 was about two times higher than that of CH_4 because the bond dissociation energy (BDE) of C_2H_6 (4.35 eV) is lower than that of CH_4 (4.55 eV) [35], resulting in the molecules of C_2H_6 being easily converted to other reactive species when compared with those of CH_4. Figure 3.5(b) shows that the main gaseous products are only H_2, C_2H_4, and C_2H_2 with trace amounts of C_3H_8 and C_4H_{10}. Again, no other products of higher C_4 hydrocarbons were detected. Figure 3.5(c) shows the product selectivities and the molar ratios of H_2/C_2H_4, H_2/C_2H_2, and C_2H_4/C_2H_2 as a function of feed flow rate. With increasing feed flow rate, the selectivities for H_2 and C_2H_2 tended to decrease slightly. In contrast, the selectivity for C_2H_4 increased prominently, but the selectivities for C_3H_8 and C_4H_{10} remained unchanged with increasing feed flow rate. The molar ratio of H_2 to C_2H_2 or C_2H_4 tended to decrease slightly, while the C_2H_4/C_2H_2 molar ratio increased with increasing feed flow rate, suggesting that the rate of the dehydrogenation reaction decreases with increasing feed flow rate.

In a comparison with the CH_4/He feed system at any given feed flow rate, the addition of C_2H_6 showed experimentally the increment of CH_4 conversion,

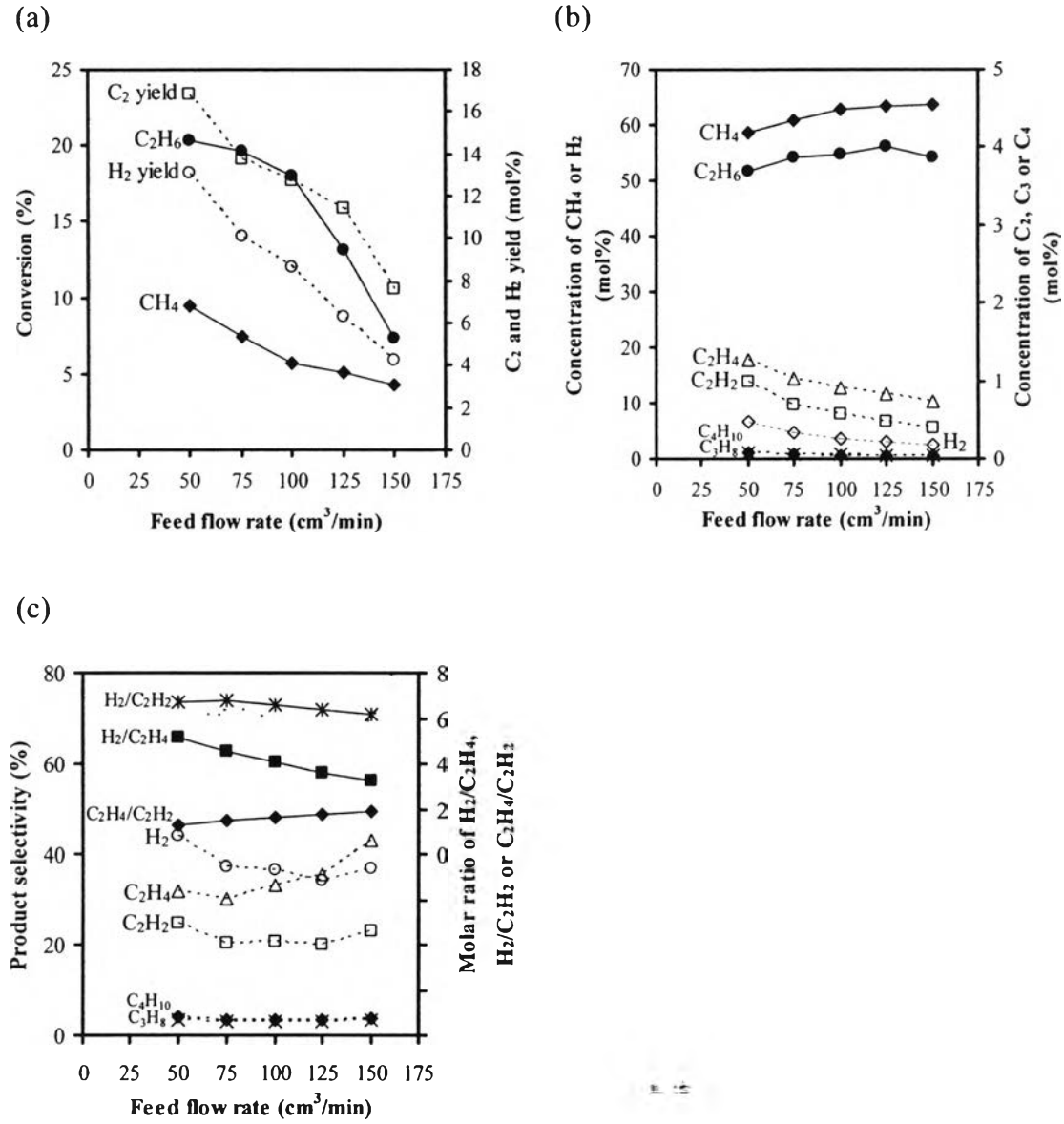

Figure 3.5 Effect of feed flow rate on (a) reactant conversions and product yields, (b) concentrations of outlet gas, and (c) product selectivities of methane/ethane/helium feed system (applied voltage, 15.5 kV; frequency, 200 Hz; and electrode gap distance, 6 mm).

especially at low feed flow rates. Thanyachotpaiboon *et al.* [36] also described the enhancement of CH_4 conversion in the case of adding ethane to the feed and using a DBD reactor where the ethane-derived active species are able to activate methane more readily than those formed from methane itself. Conversely, at a higher flow rate, the CH_4 conversion was found to be lower than that of the CH_4/He feed system,

indicating that adding ethane does not promote the synergetic effect on the CH_4 conversion at these conditions of high feed flow rates. It is believed that a number of highly energetic electrons collide with ethane instead of methane, and some radicals dissociated from ethane may form methane, thus allowing for a lowering of the CH_4 conversion. Furthermore, the addition of C_2H_6 can somewhat enhance the extent of product concentrations, particularly H_2 and C_2 products. As can be seen in Figure 3.5(c), the selectivities for C_3H_8 and C_4H_{10} remain almost unchanged for all feed flow rates. Meanwhile, the C_2H_4 selectivity increased while the selectivities for C_2H_2 and H_2 decreased slightly with increasing feed flow rate. Because some quantities of C_2H_2 and H_2 produced in this feed system are generated from the dehydrogenation reactions of C_2H_4, the rate of C_2H_4 dehydrogenation becomes lower with the increasing feed flow rate, which is confirmed from the decrease in the H_2/C_2H_4 molar ratio from 5.18 to 3.28, as well as the increase in the C_2H_4/C_2H_2 molar ratio from 1.29 to 1.89. The product distribution of the CH_4/C_2H_6/He feed system had quite similar trends to that of the CH_4/He feed system, as described above. However, higher quantities of H_2, C_2H_4, C_2H_2, C_3H_8, and C_4H_{10} selectivities are clearly noticed in this feed system, suggesting that the presence of C_2H_6 in the gas feed mixture enhances the plasma reactions. Similarly, Thanyachotpaiboon *et al.* [36] found that higher selectivities for C_3 and C_4 hydrocarbons could be obtained by the addition of C_2H_6 in the feed. Surprisingly, the amount of carbon deposit was not apparently different from that of the pure methane feed system, although the CH_4/C_2H_6/He feed system had a lower partial pressure of methane due to the dilution by the addition of He and C_2H_6 in the feed. The results indicate that carbon deposit may be not only derived from the cracking reaction of methane, but may also result from the cracking reaction of ethane.

3.4.4 $CH_4/C_2H_6/C_3H_8$/He Feed System

In this experiment, 5% propane was introduced into the feed gas mixture in order to investigate the effect of added propane on the reforming of methane under a plasma environment with a molar ratio of the CH_4:C_2H_6:C_3H_8:He feed system of 70:5:5:20. The results of the $CH_4/C_2H_6/C_3H_8$/He feed system at various feed flow rates in the range of 75-175 cm^3/min are presented in Figure 4.6.

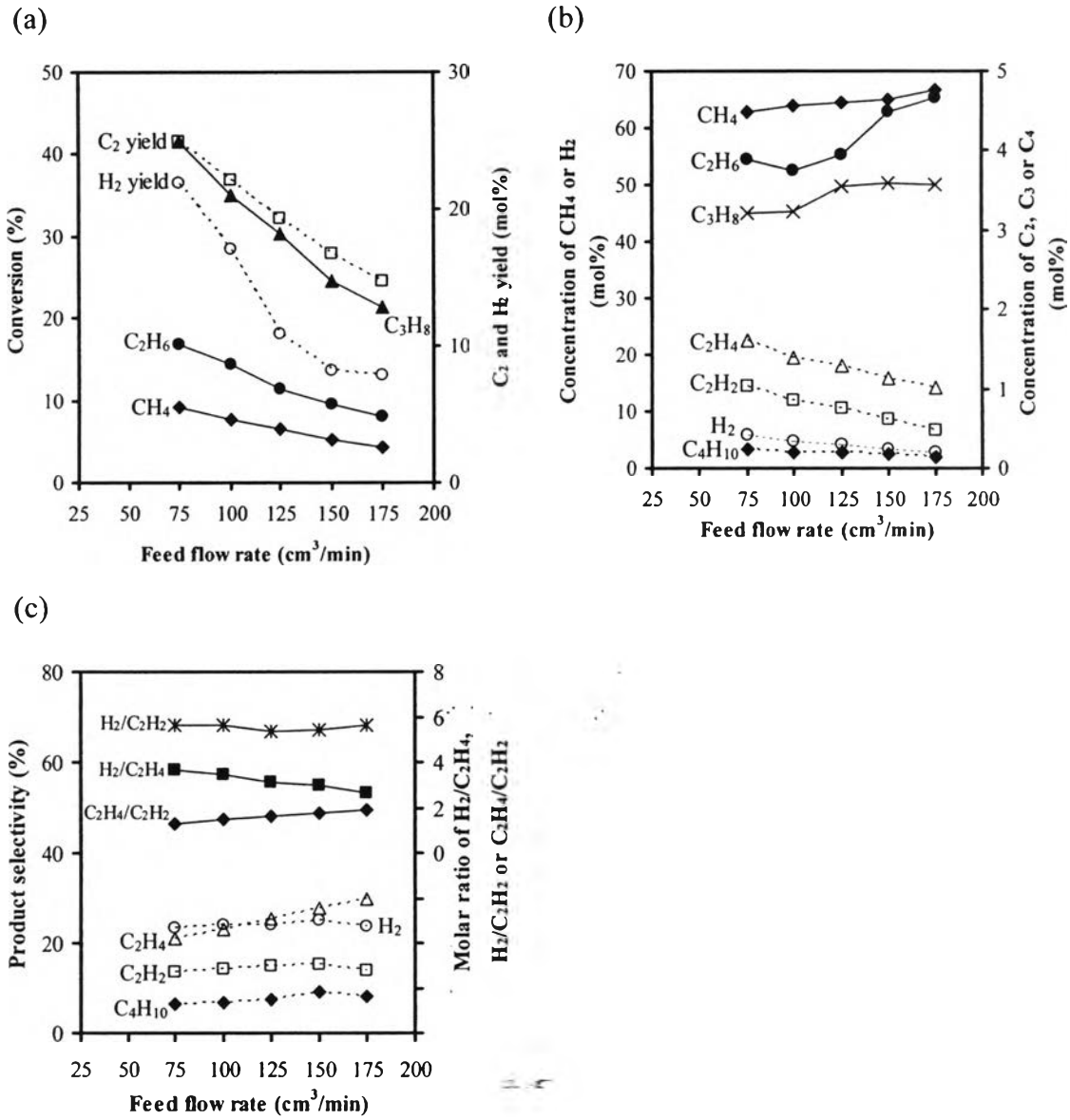

Figure 3.6 Effect of feed flow rate on (a) reactant conversions and product yields, (b) concentrations of outlet gas, and (c) product selectivities of methane/ethane/propane/helium feed system (applied voltage, 15.5 kV; frequency, 200 Hz; and electrode gap distance, 6 mm).

Both the conversions of three hydrocarbon reactants (CH_4, C_2H_6, and C_3H_8) and the product yields (H_2 and C_2) are significantly influenced by the feed flow rate, as shown in Figure 3.6(a). With increasing feed flow rate, from 75 to 175 cm^3/min, the CH_4 conversion slightly decreased from 9.23 to 4.38%, the C_2H_6 conversion moderately decreased from 21.90 to 7.83%, and the C_3H_8 conversion drastically

dropped from 41.54 to 21.39%. As mentioned before, the effect of feed flow rate is clearly affected by the residence time. From the results, the reactant conversions were in the following order: $C_3H_8 > C_2H_6 > CH_4$. The results can be explained by the differences in the bond dissociation energies of propane, ethane and methane, which are 4.33, 4.35 and 4.55 eV, respectively [35]. The effect of feed flow rate on the outlet gas composition is shown in Figure 3.6(b). Both C_2H_2 and C_2H_4 concentrations declined remarkably when the feed flow rate increased. The concentrations of H_2 and C_4H_{10} decreased slightly with increasing feed flow rate. The concentration of H_2 was in the range of about 2-6%, which is equivalent to 8-17% H_2 yield. From Figure 3.6(c), when the feed flow rate increases, the C_2H_4 selectivity increases from 20.88 to 29.96% while the selectivities for H_2, C_2H_2, and C_4H_{10} remain nearly invariant for all feed flow rates. Also, the molar ratio of H_2 to C_2H_4 decreased, but the molar ratio of C_2H_4 to C_2H_2 increased with an increment of feed flow rate. The molar ratio of H_2 to C_2H_2 was nearly unaffected by changes in the feed flow rate.

For a comparison between the CH_4/C_2H_6/He and $CH_4/C_2H_6/C_3H_8$/He feed systems, the latter system had concentrations of all products higher than in the former system, suggesting that the addition of C_3H_8 simply enhances all plasma reactions. Moreover, a much larger amount of coke was found to deposit on the electrode surface and the reactor inner wall, indicating a higher amount of carbon deposit derived primarily from the cracking reactions of all reactants: methane, ethane, and propane. Interestingly, the results of all product selectivities of the $CH_4/C_2H_6/C_3H_8$/He feed system were lower than the CH_4/C_2H_6/He feed system, except for the C_4H_{10} selectivity. A possible explanation is that C_3H_8 added to the feed requires more energy in order to be converted into smaller compounds (e.g. carbon, C_2 hydrocarbons and H_2) via the dissociation, coupling, dehydrogenation, and cracking reactions. Besides, some extent of formed products may be reformed to reactants via recombination reactions, causing the decrement of their overall selectivities. The results reveal that the addition of He can enhance all plasma reactions pronounced than that presented in this work.

3.4.5 $CH_4/C_2H_6/C_3H_8/CO_2$ Feed System

This experiment was to investigate the effect of added CO_2 on the plasma reactions of methane reforming. The studied feed composition had a CH_4:C_2H_6:C_3H_8:CO_2 molar ratio of 70:5:5:20, which was simulated on the basis of an actual natural gas containing a high CO_2 content. For this feed system, the gilding arc system had to be run at a frequency of 300 Hz since at a frequency of 200 Hz, steady plasma could not appear for a wide range of feed flow rate (At a frequency of 200 Hz, steady plasma could only appear for a narrow range of feed flow rate from 100 to 150 cm^3/min). The results shown in Figure 3.7 present the influence of feed flow rate on the plasma reforming reactions of the simulated natural gas. From Figure 3.7(a), the conversions of all gas reactants in the simulated natural gas and product yields are influenced by feed flow rate in the studied range of 75-200 cm^3/min. The conversions of all reactants decreased with increasing feed flow rate due to the decrease in the contact time or the residence time. The propane conversion decreased substantially with increasing feed flow rate while the conversions of methane and CO_2 tended to decrease slightly. The conversions of all reactants were in the following order: C_3H_8 > C_2H_6 > CH_4 > CO_2, resulting from their bond dissociation energies, which are 4.33, 4.35, 4.55 and 5.52 eV, respectively [35]. A higher bond dissociation energy leads to more difficulty to dissociate and react to form other species. From Figure 3.7(b), the concentrations of almost all products in the plasma reactor outlet stream appear to be nearly independent of the feed flow rate. The CO_2 concentration in the outlet gas stream only slightly dropped from its initial concentration. The amount of hydrogen produced was approximately 4-6%, corresponding to 8-17% H_2 yield. Likewise, the product selectivities for C_2H_4, H_2, C_2H_2, C_4H_{10} and CO remain almost unchanged with the feed flow rate, as shown in Figure 3.7(c). Similar to the results of product selectivities, the product molar ratios were not affected by the feed flow rate. The H_2/CO and (C_2H_4+C_2H_2)/CO molar ratios were relatively constant at approximately 13-14 and 6-7, respectively. The molar ratio of H_2/CO was approximately twice that of (C_2H_4+C_2H_2)/CO. This can be explained in that both the dissociation reactions and the dehydrogenation reactions produce hydrogen.

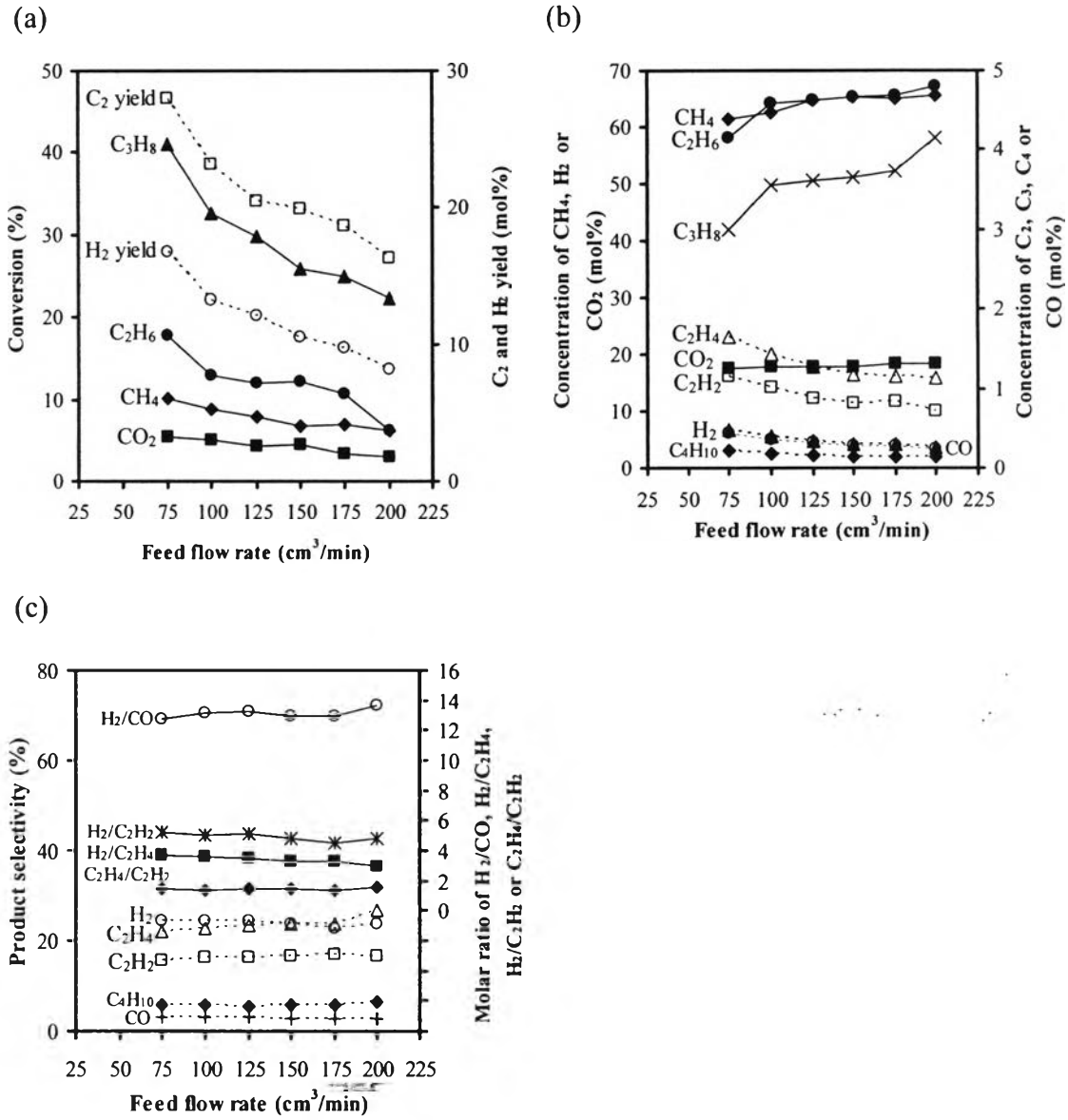

Figure 3.7 Effect of feed flow rate on (a) reactant conversions and product yields, (b) concentrations of outlet gas, and (c) product selectivities of methane/ethane/propane/carbon dioxide feed system (applied voltage, 15.5 kV; frequency, 300 Hz; and electrode gap distance, 6 mm).

3.4.6 Comparative Results of Different Feed Gas Compositions

To gain a more qualitative understanding, the comparative results of plasma reforming reactions under different feed compositions and different feed flow rates (100, 125 and 150 cm^3/min) at an applied voltage of 15,500 V, a frequency of 200 Hz, and a gap distance of 6 mm are summarized in Figures 3.8-3.10. From

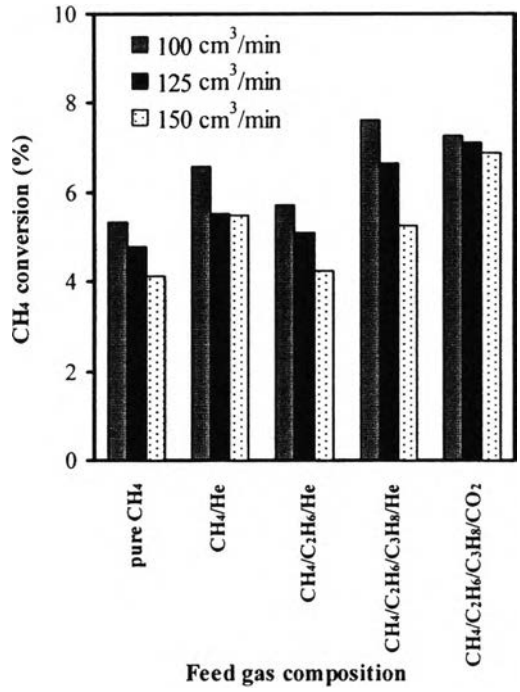

Figure 3.8 Comparison of CH_4 conversion in the different feed compositions (applied voltage, 15.5 kV; frequency, 200 Hz; and electrode gap distance, 6 mm).

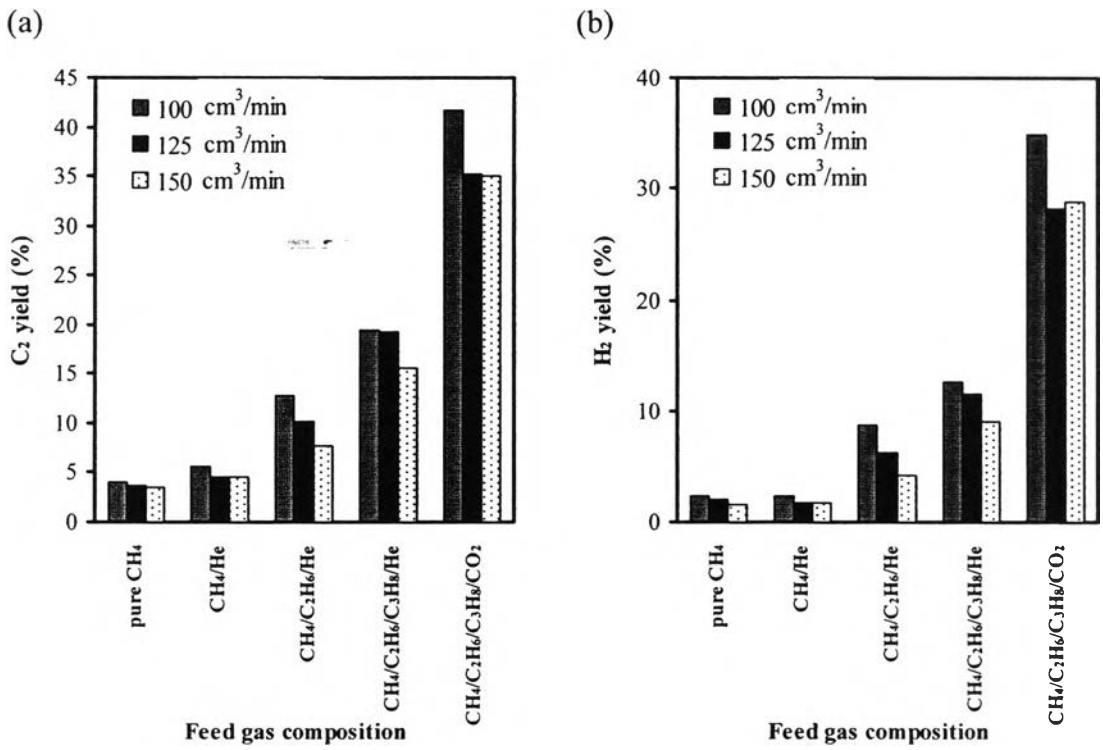

Figure 3.9 Comparison of (a) C_2 and (b) H_2 yields in the different feed compositions (applied voltage, 15.5 kV; frequency, 200 Hz; and electrode gap distance, 6 mm).

Figures 3.8 and 3.9, for any given feed system, with increasing feed flow rate, both the CH_4 conversion and the product yields clearly decrease because of decreasing residence time, as mentioned earlier. In a comparison between the pure methane and CH_4/He systems, the addition of helium resulted in the enhancement of methane conversion.

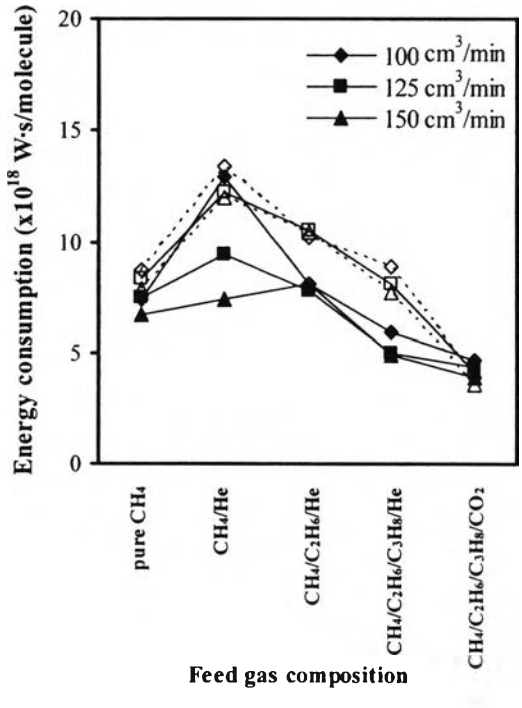

Figure 3.10 Comparison of specific energy consumption in the different feed compositions (solid line: energy consumption per reactant molecule converted; dotted line: energy consumption per hydrogen molecule produced) (applied voltage, 15.5 kV; frequency, 200 Hz; and electrode gap distance, 6 mm).

For a comparison between the pure methane and CH_4/He feed systems, the CH_4 conversion and C_2 yield were somewhat higher in the case of adding helium to the methane feed while the H_2 yield showed no difference, as compared at the same feed flow rates. An explanation for this obtained result was already reported in the previous section. In contrast, the entire system, in the case of adding He, consumed much higher energy per molecule of reactant converted or per molecule of hydrogen produced than the pure methane feed, as shown in Figure 3.10. It is partly because helium is an inert gas component that can absorb some of the

input energy, thereby leading to the higher energy consumption in the CH_4/He system. It can be concluded from these results that the addition of helium sufficiently enhances the CH_4 conversion and C_2 yield, but it causes a great increase in the specific energy consumption. When ethane is added, the CH_4 conversion decreases slightly, indicating that adding ethane does not promote the synergetic effect on the conversion of CH_4. It is believed that a number of highly energetic electrons collide with ethane instead of methane while to some extent, the radicals dissociated from ethane may form methane, therefore resulting in the insignificant change in the CH_4 conversion. In contrast to the present result, Thanyachotpaiboon *et al.* [36] reported that the CH_4 conversion increased when ethane was added in a dielectric barrier discharge (DBD) reactor. Interestingly, for the case of propane addition, a large increase in CH_4 conversion was observed. Moreover, the $CH_4/C_2H_6/C_3H_8/CO_2$ feed system exhibited very high values of CH_4 conversion at all feed flow rates and seemed to be higher than other studied feed systems without adding CO_2, particularly at high feed flow rates. In the presence of CO_2 in the feed under the plasma environment, CO_2 acts as an oxidative gas which can contribute one of two oxygen atoms for the conversion of hydrocarbons by the dissociation reactions (Equations 3.23 and 3.24). Afterwards, the active oxygen species derived from the CO_2 dissociation reactions will extract hydrogen from the molecules of hydrocarbon gases via the oxidative dehydrogenation reactions (Equations 3.25-3.30). Therefore, the addition of CO_2 considerably enhances the conversions of hydrocarbons in the feed.

Dissociation reactions of carbon dioxide;

$$e^- + CO_2 \rightarrow CO + O^- \quad (3.23)$$

$$e^- + CO_2 \rightarrow CO + O + e^- \quad (3.24)$$

Oxidative dehydrogenation reactions;

$$CH_4 + O \rightarrow CH_3 + OH \quad (3.25)$$

$$C_2H_6 + O \rightarrow C_2H_5 + OH \quad (3.26)$$

$$C_3H_8 + O \rightarrow C_3H_7 + OH \quad (3.27)$$

$$CH_4 + OH \rightarrow CH_3 + H_2O \quad (3.28)$$

$$C_2H_6 + OH \rightarrow C_2H_5 + H_2O \quad (3.29)$$

$$C_3H_8 + OH \rightarrow C_3H_7 + H_2O \quad (3.30)$$

Regarding the results of H_2 and C_2 yields as shown in Figure 3.9, at any given feed flow rate, the $CH_4/C_2H_6/C_3H_8/CO_2$ feed system provides the highest H_2 yield, as well as the highest C_2 yield, while the CH_4/He feed system gives the lowest H_2 yield. As noted earlier, the CO_2 added to the feed can extract hydrogen atoms form the molecules of hydrocarbons, thereby providing more opportunities for coupling reactions to occur. In addition, H_2 molecules could also be obtained from the dehydrogenation reactions of C_2H_6 and C_3H_8. For the CH_4/He feed system, H_2 formation seems to be less than other feed systems, resulting from the reactant gas component as the source of hydrogen being only methane.

The energy consumption of the AC gliding arc system is very complex, depending on the composition of feed gas and the reaction products in the plasma zone. As compared in Figure 3.10, which shows the energy consumption per reactant molecule converted or per hydrogen molecule produced in the different feed compositions at various feed flow rates, the quantities of specific energy consumption are clearly seen to reduce in the following order: CH_4/He > CH_4/C_2H_6/He > $CH_4/C_2H_6/C_3H_8$/He > $CH_4/C_2H_6/C_3H_8/CO_2$ feed gas systems. For the different feed compositions studied, the minimum energy requirement was found for $CH_4/C_2H_6/C_3H_8/CO_2$ feed system to be about 3.86×10^{-18}- 4.63×10^{-18} W·s (24.08-28.92 eV) per molecule of converted reactant and 3.58×10^{-18}- 4.14×10^{-18} W·s (22.35-25.82 eV) per molecule of produced hydrogen.

3.5 Conclusions

The conversion of natural gas containing a high concentration of carbon dioxide and other hydrocarbon gas components was investigated at various feed flow rates under non-thermal gliding arc discharge plasma. The major products were hydrogen and C_2 hydrocarbons with high product yields and product selectivities. The presence of other gas components presented in natural gas was found to play an important role affecting the reaction performance, the chemical reaction pathways and the plasma stability. For all added gaseous components, including ethane, propane and carbon dioxide, the hydrogen and C_2 yields and specific energy consumption were found to increase significantly. In particular, the addition of

carbon dioxide provided the best results for the plasma reforming reactions of natural gas, with the highest CH_4 conversion and H_2 and C_2 product yields, and the lowest energy consumption. Further studies are currently being conducted to optimize the process parameters (applied voltage and frequency) for the reforming of natural gas with a high CO_2 content.

3.6 Acknowledgements

The authors thank the Commission on Higher Education and the Postgraduate Education and Research Program in Petroleum and Petrochemical Technology (PPT Consortium) under the Ministry of Education, Thailand, and the Research Unit of Petrochemical and Environmental Catalysis under the Ratchadapisek Somphot Endowment Fund, Chulalongkorn University, Thailand, for providing research facilities and financial support, respectively.

3.7 References

1. J.S. Chang, S.E. Park, H. Chon, Appl. Catal. A: Gen. 145 (1996) 111-124.
2. H.Y. Wang, E. Ruckenstein, Appl. Catal. A: Gen. 204 (2000) 143-152.
3. Z. Hou, O. Yokota, T. Tanaka, T. Yashima, Appl. Catal. A: Gen. 253 (2003) 381-397.
4. M.M.V.M. Souza, L.C. Clave, V. Dubois, C.A.C. Perez, M. Schmal, Appl. Catal. A: Gen. 272 (2004) 133-139.
5. H.S. Roh, H.S. Potdar, K.W. Jun, Catal. Today 93-95 (2004) 39-44.
6. H.W. Chen, C.Y. Wang, C.H. Yu, L.T. Tseng, P.H. Liao, Catal. Today 97 (2004) 173-180.
7. A. Shamsi, Appl. Catal. A: Gen. 277 (2004) 23-30.
8. O. Motret, S. Pellerin, M. Nikravech, V. Massereau, J.M. Pouvesle, Plasma Chem. Plasma Process 17 (1997) 393-407.
9. H.D. Gesser, N.R. Hunter, D. Probawono, Plasma Chem. Plasma Process. 18 (1998) 241-245.

10. O. Mutaf-Yardimici, A.V. Savaliev, A.A. Fridman, L.A. Kennedy, Int. J. Hydrogen Energy 23 (1998) 1109-1111.
11. M.A. Malik, X.Z. Jiang, Plasma Chem. Plasma Process. 19 (1999) 505-512.
12. A. Huang, G. Xia, J. Wang, S.L. Suib, Y. Hayashi, H. Matsumoto, J. Catal. 189 (2000) 349-359.
13. T. Oberreuther, C. Wolff, A. Behr, IEEE Trans. Plasma Sci. 31 (2003) 74-77.
14. Y. Zhang, Y. Li, Y. Wang, C. Liu, B. Eliasson, Fuel Process. Technol. 83 (2003) 101-109.
15. H.K. Song, H. Lee, J.W. Choi, B.K. Na, Plasma Chem. Plasma Process. 24 (2004) 57-72.
16. H.K. Song, J.W. Choi, S.H. Yue, H. Lee, B.K. Na, Catal. Today 89 (2004) 27-33.
17. S. Futamura, IEEE Member, G. Annadurai, IEEE Trans. Ind. Appl. 41 (2005) 1515-1521.
18. A. Fridman, S. Nester, L.A. Kennedy, A. Saveliev, O. Mutaf-Yardimci, Prof. Energ. Combust. 25 (1999) 211-231.
19. A. Fridman, L.A. Kennedy, Plasma physics and engineering, Taylor & Francis, New York, 2004.
20. K. Krawczyk, M. Młotek, Appl. Catal. B: Environ. 30 (2001) 233-245.
21. D. Moussa, J.L. Brisset, J. Hazard.Mater. 102 (2003) 189-200.
22. F. Abdelmalek, S. Gharbi, B. Benstaali, A. Addou, J.L. Brisset, Water Res. 38 (2004) 2339-2347.
23. M. Moreau, N. Orange, J.L. Brisset, Ozone Sci. Eng. 27 (2005) 469-473.
24. R. Burlica, M.J. Kirkpatrick, B.R. Locke, J. Electrostat. 64 (2006) 35-43.
25. J. Janca, A. Czernichowski, Surf. Coat. Tech., 98 (1998) 1112-1115.
26. J. Janca, P. Stahel, J. Buchta, D. Subedi, F. Krcma, Pryckova. Plasmas Polym. 6 (2001) 15-26.
27. B. Benstaali, A. Addou, J.L. Brisset, Mater. Chem. Phys. 78 (2002) 214-221.
28. A. Czernichowski, Oil Gas Sci. Technol. 56 (2001) 181-198.
29. I. Rusu, J.M. Cormier, Chem. Eng. J. 15 (2003) 23-31.
30. A. Indarto, J.W. Choi, H. Lee, H.K. Song, J. Nat. Gas. Chem. 14 (2005) 13-21.
31. T. Paulmier, L. Fulcheri, Chem. Eng. J. 106 (2005) 59-71.

32. A. Indarto, J.W. Choi, H. Lee, H.K. Song, Energy 31 (2006) 2986-2995.
33. A. Holmen, O. Olsvik, O.A. Rokstad, Fuel Process Technol. 42 (1995) 249-267.
34. T. Sreethawong, P. Thakonpatthanakun, S. Chavadej, Int. J. Hydrogen Energy 32 (2007) 1067-1079.
35. J.A. Dean, Lange's handbook of chemistry, fifteenth ed., McGraw-Hill, New York, 1999.
36. K. Thanyachotpaiboon, S. Chavadej, L. Caldwell, L.L. Lobban, R.G. Mallinson, AIChE J. 44 (1998) 2252-2257.